# A Novel Two-terminal Fault Location Approach Utilizing Traveling-waves for Series Compensated Line Connected to Wind Farms

Saswati Mishra, Shubhrata Gupta, Anamika Yadav

***Abstract*—In this paper, a novel two-terminal fault location approach utilizing traveling-waves for series compensated transmission line connected to wind farms is presented. The approach is based on accurate estimation of arrival time of waves (ATWs) at both ends of the line. The first step in estimation of ATWs is the application of estimation of signal parameters via rotational invariant techniques (ESPRIT) on three-phase instantaneous voltage signals measured at both ends of the line after inception of fault in order to obtain reconstructed signals. The next step of the approach involves calculation of errors between aerial-modes of original and reconstructed signals (obtained via ESPRIT). Finally, the peak of squared-errors are utilized to determine ATWs. The simulation is carried out in PSACAD/EMTDC environment on IEEE-14 bus test system with a line having 50 % series compensation connected to 300 MW wind farm. The efficacy of FLE approach is validated under different fault scenarios and found to be accurate regarding fault location estimation.**

***Keywords*—Arrival time of waves, DFIG-based wind farm, ESPRIT, fault location, series compensation.**

## I. Introduction

MODERN day power networks are expanding at a faster rate in order to meet increasing power demand [1]. Wind energy integration into existing system and incorporation of series compensation to enhance transmission capacity are presently preferred trends adopted by electric utility [2], [3]. The aforementioned trends are preferred due to associated technical and economic benefits. Basically, doubly-fed induction generators (DFIG) based wind farms are utilized for wind energy integration. However, the control strategy of DFIG-based wind farms and series compensation may vary the transmission line impedance during both steady-state as well as transient operation of the system [4]. The control strategies of DFIG-based wind farms and of series compensation introduce changes in the system parameters like load currents and bus voltages. Aforementioned variations in system parameters consequently affect the calculated line impedance. This phenomenon is more prominent when the system is subjected to transient operation. When wind farm and series compensation both are incorporated in a transmission line then, the complexity of the system increases significantly. As a matter of consequence, the traditional transmission line protection schemes may fail to operate securely and reliably [5].

In case of systems experiencing faults, the secure and reliable operation depends a lot on proper power system restoration within minimum possible time. Accurate fault location estimation (FLE) is a vital factor which helps in faster restoration process. FLE approaches reported in literature can be broadly classified into three categories: impedance-based; artificial intelligence-based; and traveling wave-based methods [6]. Impedance-based methods are simple but need accurate modeling of power networks in order to achieve efficient fault location estimation. However, the occurrence of undesired and critical power system conditions like generating unit outages, transmission line faults, load encroachment, power swing etc. may lead inaccurate modeling of the system eventually affecting the reliability of impedance-based methods. On the other hand, artificial intelligence-based methods are complex and computationally inefficient which narrow down their possibility of practical implementations. Moreover, traveling wave-based methods overcome the disadvantages associated with impedance-based and artificial-based methods [6]. Traveling wave-based techniques estimate arrival time of waves (ATWs) from voltage or current signals measured at the ends of the transmission line after the inception of fault and utilize the estimated ATWs in fault location estimation. Therefore, accurate modeling of power system in not required for their implementation. Further, these methods are practically implemented with the aid of modern day advanced communication infrastructure.

As mentioned earlier that traveling wave-based methods estimate ATWs from the measured signals (voltage or current) at ends of line so their accuracy depends on the measured signals. It is well known that wind integration utilizes power electronics equipment for injecting power to grid which eventually affect the quality of injected power (presence of harmonics and inter-harmonics) [7]. Consequently, the efficiency of traveling wave methods using these injected signals get worsened. Further, series compensation affects the voltage and current signals measured at terminals of the line and this too deteriorate the efficiency of traveling wave-based methods [6]. Therefore. it is required to develop a robust traveling wave-based FLE approach which remains insensitive towards series compensation and wind integration. Further, limited research are available in literature regarding development of robust FLE approach for the series compensated system connected or not connected to wind farms

S. Mishra, S. Gupta and A. Yadav are with the department of Electrical Engineering, National Institute of Technology, Raipur, CG 492099 INDIA(e-mail of corresponding author: saswatimishra2015@gmail.com).

Paper submitted to the International Conference on Power Systems Transients (IPST21) in Belo Horizonte, Brazil June 06-21, 2021.

[4], [8], [9], [10], [11], [12]. Aforementioned facts motivated the authors to carry out present work of developing a novel two-terminal FLE approach utilizing traveling waves for the mentioned system.

## II. Background and Contribution

In past decades, several attempts are undertaken by power system protection research community towards providing secure and reliable transmission line protection schemes to the series compensated lines connected or not connected to wind farms [8], [9], [10], [11], [12]. A brief overview of reported works are presented below.

In [4], a protection and location scheme based on fast discrete S-transfrom (FDST) is presented for series compensated line connected to wind farm. In [13], a fast discrete orthogonal S-transform (FDOST) is used to classify faults in series compensated system. FDOST algorithm is utilized for developing protection scheme for TCSC compensated system in [14]. However, S-transform and its different variants suffer from poor time-frequency resolution resulting in erroneous estimation of fault location [6]. Artificial intelligence based FLE approaches utilizing artificial neural network (ANN), wavelet transform (WT), discrete WT (DWT) and decision tree are used to locate faults in series compensated lines [10], [11], [12]. ANN is complex and computational burden is high which limits its practical implementation. Further, the performance of WT and DWT depends a lot on the choice of mother wavelets and the level of decomposition of signals [15]. In [16], fault localization is carried out using negative-sequence phasors for series compensated system. However, the method may produce inaccurate fault location estimation under critical power conditions due to inappropriate calculation of phasors. A fast transmission line protection scheme utilizing current samples is proposed for line connected to wind farms in [17]. In [18], an adaptive transmission line protection scheme is proposed for wind integrated system. The transmission line protection scheme is based on adjusting relay trip characteristics from local end information. The direction of flow of currents are used for transmission line protection scheme of line connected to wind farms [19]. The efficiency of above methods may deteriorate in critical power system conditions since current signals are more sensitive towards transient phenomenon. In [20], the polarity of positive-sequence current is utilized to protect line connected to wind farms using empirical mode decomposition (EMD). EMD experiences shift insensitivity and poor time-frequency resolution which make it less reliable method [6]. To identify shunt faults in lines, an adaptive transmission line protection scheme is proposed is [21]. An optimization approach is adopted to set adaptive threshold for system of wind farm connected line in [22]. In [23], a protection scheme for wind integrated transmission system against balanced faults is presented. A differential equation approach in time-domain is utilized for protection of wind farm connected lines in [24]. However, time-domain approaches require accurate system modeling in order to perform efficiently. In [25], different studies for efficient protection for DFIG-based wind farms are presented. Mitigation techniques for affected protection system of wind farm connected lines are presented in [26]. A review on traveling wave based protection schemes for renewable penetrated systems is presented in [27].

The prime focus of aforementioned studies are on proposing fast protection scheme for lines connected to wind farms. Further, few reports are available on protection of series compensated line connected to wind farms. In addition to above observations, it can be clearly noticed that development of FLE approaches for series compensated line connected to wind system are least attended area of research. However, owing to complexity of present power system structures, it is necessary to develop an efficient FLE approach for fast and reliable power system restoration. The above stated fact primarily motivated the authors to propose a novel FLE approach for series compensated transmission system with wind penetration.

In this work, a two-terminal traveling wave based FLE approach is presented. In this method, estimation of signal parameters via rotational invariant techniques (ESPRIT) is used to reconstruct three-phase instantaneous terminal bus voltages measured at the ends of line. The error between aerial-modes of original and reconstructed signal is calculated and ATW is estimated from the instant of peak of squared-error signal. The estimated ATWs are then used to localize the faults. The efficacy and robust performance of the proposed FLE approach is validated on standard IEEE-14 bus test system with wind integration and series compensation. The major contributions of the work are highlighted below.

- A novel two-terminal fault location approach utilizing traveling waves for series compensated line connected to wind farms is presented in this work.
- The peak of the squared error signal obtained from aerial-modes of original and reconstructed signal (via ESPRIT) is used to estimate ATWs.
- Different test cases are simulated to establish the robust performance of FLE approach.

The novelty of present work are the application of ESPRIT in detection of traveling waves at the bus terminals and estimation of ATWs from the instant of peak of squared error found between aerial modes of original and reconstructed (via ESPRIT) terminal voltages.

The rest of the paper is organized as follows. Section II highlights the background of present work along with contribution. Section III presents preliminaries of ESPRIT algorithm. The details of modeled system is presented in Section IV. The ESPRIT based proposed FLE approach is described in Section V. Simulation results followed by discussion are presented in Section VI. Finally, Section VII concludes the work with scope of future.

## III. Preliminaries

In this section, an overview of ESPRIT algorithm is presented. The algorithm is introduced as an alternative to direction of arrival (DOA) estimation method [28]. It is an subspace analysis based algorithm used to estimate the

parameters (i.e amplitude, phase, decay and frequency) of a signal. This algorithm offers several advantages over other parametric methods like efficient estimation and high accuracy [29].

Consider a signal $s[n]$ of length $N$ represented in following form

$$s[n] = \sum_{k=1}^{K} \alpha_k v(f_k) e^{j2\pi n f_k} + \mathbf{w}[n] = \mathbf{V}\Phi^n \alpha + \mathbf{w}[n] \quad (1)$$

where $\mathbf{V}$ is $N \times P$ constructed from frequency vectors $v(f_k) = [1\ e^{j2\pi f_k}\ e^{j4\pi f_k}\ \cdots\ e^{j2\pi(N-1)f_k}]^T$ of length $N$ corresponding to $K$ frequencies and $\mathbf{V} = [v(f_1)\ v(f_2)\ \cdots\ v(f_k)]$. $\alpha$ is a vector made up of amplitudes of each $\alpha_k$ i.e. $\alpha = [\alpha_1\ \alpha_2\ \cdots\ \alpha_k]^T$. $\Phi$ is a diagonal matrix of shifted phase between consecutive time samples of components of $s[n]$. $\mathbf{w}[n]$ is a vector of noise.

$$\Phi = \mathbf{diag}[\phi_1\ \phi_2\ \cdots\ \phi_k] = \begin{bmatrix} e^{j2\pi f_1} & 0 & \cdots & 0 \\ 0 & e^{j2\pi f_2} & \cdots & 0 \\ \vdots & \vdots & \ddots & \vdots \\ 0 & 0 & \cdots & e^{j2\pi f_k} \end{bmatrix} \quad (2)$$

It can be noticed that $\Phi$ is a rotation matrix and thus, it is used by ESPRIT to estimate the frequency components. Suppose there are two overlapping sub-windows $S_{N-1}[n] nad S_{N-1}[n+1]$ of length $N-1$ within time-indexed vector of length $N$ represented in following manner

$$s[n] = \begin{bmatrix} s_{N-1}[n] \\ s[n+N-1] \end{bmatrix} = \begin{bmatrix} s[n] \\ s_{N-1}[n+1] \end{bmatrix} \quad (3)$$

Mathematically, $s_{N-1}[n]$ which is a sub-window of length $(N-1)$ of $s[n]$ is expressed as

$$s_{N-1}[n] = \mathbf{V}_{N-1}\Phi_n \alpha \quad (4)$$

From 4, two subspace matrices are obtained in following manner

$$\mathbf{V}_1 = \mathbf{V}_{N-1}\Phi_n \quad (5)$$

$$\mathbf{V}_2 = \mathbf{V}_{N-1}\Phi_{n+1} \quad (6)$$

From the subspace matrices obtained in 5, construct a matrix $\mathbf{A}$ as shown below.

$$\mathbf{A} = [\mathbf{V}_1] \backslash [\mathbf{V}_2] \quad (7)$$

Now, solve the left-hand eigenvalue problem as follows.

$$y = \mathbf{eig}(A) \quad (8)$$

Once, the eigenvalue problem is solved then, compute the residues $\mathbf{R}$ in following manner.

$$\mathbf{R} = [y]^{\dagger}[s] \quad (9)$$

where $\dagger$ represents the pseudo-inverse. Using above equations, parameters like amplitude, frequency, phase and decay of a signal are estimated. Using these parameters, the signal can be reconstructed.

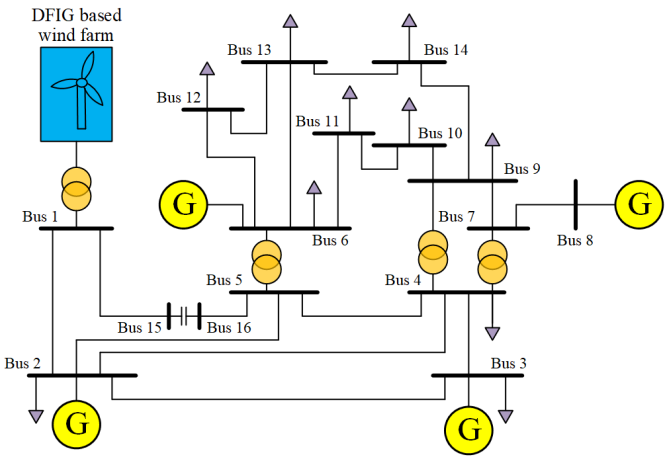


Fig. 1. Schematic of studied system.

## IV. Simulation Model

### A. Test system under study

The standard IEEE-14 bus test system is used in this work for all simulation studies. The data for the system are taken from [30]. The test system is modified by incorporating series compensation and wind integration for simulation studies in this work. PSACD/EMTDC platform is used to model the system. Fig. 1 illustrates schematic diagram of the modeled system. The synchronous generator at bus 1 is replaced by a DFIG-based wind farm of 300 MW. A compensation level of 50% is provided at the middle of 138 kV line 1-5 with the aid of a fixed capacitor of rating 105.79 $\mu$F. A distributed line parameter for the line is considered. For all simulation, the fault is assumed to be initiated on this line.

### B. Modeling of DFIG-based wind farm

An aggregated model of DFIG-based wind farm is used in this work. The schematic of a DFIG-based generating unit is illustrated in Fig. 2 (a). The unit is equipped with pitch angle control in order to balance the aerodynamic torque in case of wind speed exceeds the rated value. A crowbar protection is provided at the rotor side which gets activated in the event of over-current in rotor winding and/or over-voltage of DC link. The pulse width modulation required by rotor and grid-side converters is controlled by space vector control scheme. The wind farm consists of a total 60 generating units, each of 5 MW rated output, resulting in total capacity of 300 MW.

As mentioned earlier, the pitch angle control scheme is adopted for adjusting the wind turbine blade angle ($\beta$) for improved aerodynamic torque. The scheme controls angle with the aid of proportional–integral controller. The block diagram representation of the control scheme is depicted in Fig. 2 (b). Two controllers are used in this scheme where the input to first controller is the difference of mechanical power output of turbine ($P_m$) and reference value equal to 1.1 p.u. while the second controller takes the difference of output power of DFIG-based unit ($P_g$) and reference value of 1.0 p.u. as input. The output control signals of the controllers are summed up and fed to limiter. The final output is the pitch angle ($\beta$) to

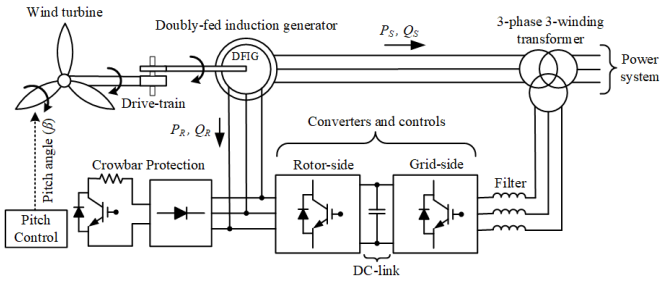


(a)

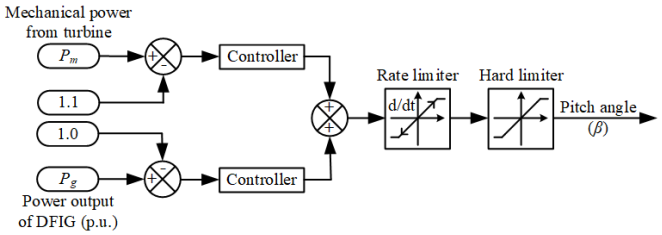


(b)

Fig. 2. Modeling and control of DFIG-based wind farm. (a) Model of wind farm. (b) Pitch control of wind turbine.

which the turbine blades are adjusted to achieve improved aerodynamic torque.

## V. Proposed FLE Approach

The proposed FLE approach is based on the fact that when a fault occurs on a line then traveling waves are generated which terminate at both ends of the line. The relays at bus terminals sense the arriving wave pulses and from this information, ATWs can be estimated. In this work, ESPRIT algorithm is used to reconstruct then signal after fault inception. The aerial-modes of original and estimated signals are obtained. The difference between two signals is the error signal. The square of this error signal is then obtained and the time corresponding to peak of the signal is designated as ATW. From the estimated ATWs, the fault location is obtained.

To demonstrate the working of proposed FLE approach, a two bus example is considered as shown in Fig. 3. A fault is assumed to be initiated at point $F$ at distance of $x$ from bus $S$ on the line $S-R$ of total length $D$. The fault waves start traveling towards both ends of the line as soon as the fault occurs at a speed $v = \frac{1}{\sqrt{LC}}$. Here, $L$ and $C$ are the inductance and capacitance of the line $S-R$, respectively. It can be observed from the figure that waves reaches the end of the line and get reflected at bus terminals and again at the fault point. Let, the first ATWs recorded at both ends of the line are $A_{T1}$ and $A_{T2}$. Accordingly, the fault location from bus $S$ is estimated by following equation.

$$EFL = \frac{D - v(A_{T2} - A_{T1})}{2} \tag{10}$$

Once the fault location is estimated, the percentage error $PE$ in FLE is obtained as

$$PE = \frac{|AFL - EFL|}{D} \times 100 \tag{11}$$

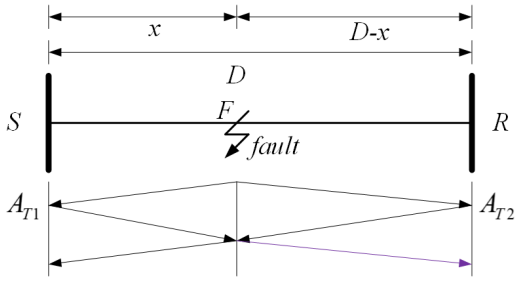


Fig. 3. Schematic of studied system.

TABLE I
Distributed Line Parameters

| Parameter | Value (pu/m) |
|---|---|
| Positive-sequence resistance $R$ | 0.05403e-5 |
| Positive-sequence reactance $X_L$ | 0.22304e-5 |
| Postive-sequence susceptance $B$ | 0.04920e-5 |

As mentioned above that in proposed FLE approach, the aerial mode of the signals is first obtained from the original and reconstructed three-phase signals. This is accomplished by using Clarke's transformation [6]. Then, error signal is obtained from the difference of the two signals. Further, ATWs are estimated from the squared error signals. Fig. 4 demonstrates estimation of ATWs from three-phase voltage signals measured at bus $S$. A three-phase fault is assumed to be initiated at 0.6 s. The signals are sampled at 1000 kHz sampling frequency. For estimation of ATWs, (3/10) post-fault samples are considered. In Fig. 4 (a), original three-phase voltage signal is shown while the reconstructed signal (via ESPRIT) is shown in Fig. 4 (b). The aerial-mode of the signals is obtained by Clarke's transform and is illustrated in Fig. 4 (c). Fig. 4 (d) shows the plot of squared-error signal. From the plot, ATW is estimated from the peak of the signal as shown. Similarly, ATW is estimated for the signal at other end of the line i.e. bus $R$. Fig. 5 illustrates the estimation of ATW at bus B2. The detailed proposed FLE approach is depicted by flowchart shown in Fig. 6.

## VI. Numerical Results and Discussion

To validate the efficient and robust performance of the proposed FLE approach, several test conditions of different fault scenarios are simulated. In all cases, different types of shunt faults are initiated on the line 1-5 at 0.5 s. The length of line is considered to be 200 km. The fundamental frequency of the system is 60 Hz and the sampling frequency is taken equal to 1000 kHz. The detailed test cases are discussed in following subsections. The distributed line parameters are considered for modeling the transmission line. The values of parameters are listed in Table I.

### A. Performance under different fault scenarios

In this section, the performance of proposed FLE approach is validated for different fault scenarios. The fault resistance (FR) is varied from 0.01 to 5 Ω and fault inception angle

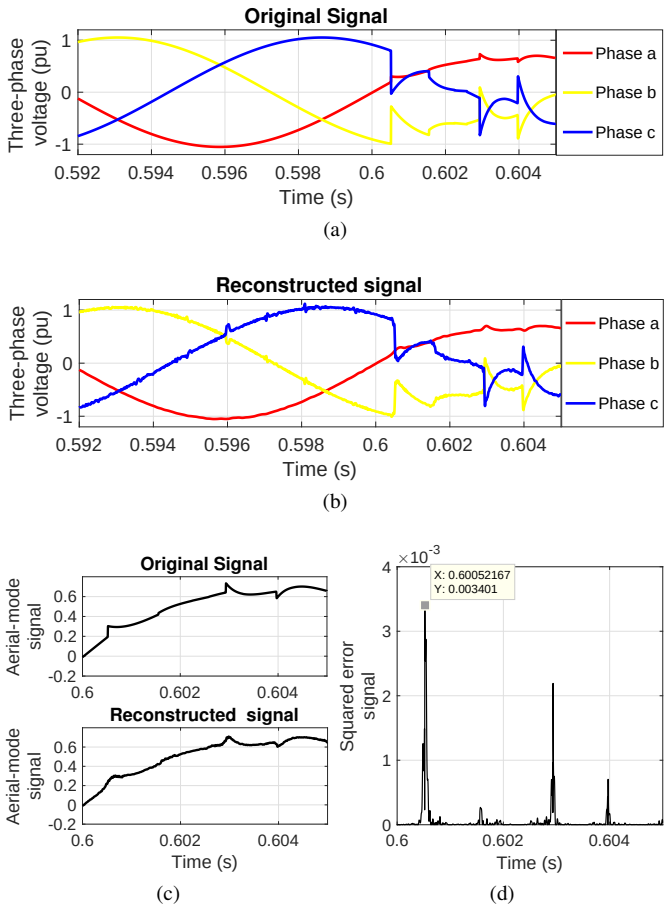


Fig. 4. Estimation of ATWs at bus $S$. (a) Original three-phase voltage signal. (b) Reconstructed three-phase voltage. (c) Aerial-mode of the signals. (d) Squared-error signal.

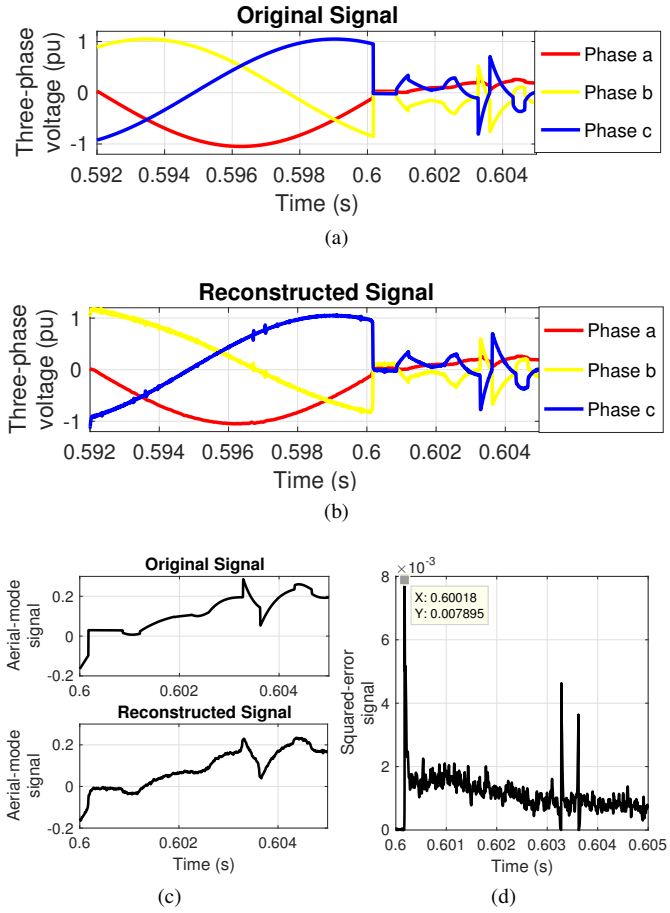


Fig. 5. Estimation of ATWs at bus $R$. (a) Original three-phase voltage signal. (b) Reconstructed three-phase voltage. (c) Aerial-mode of the signals. (d) Squared-error signal.

(FIA) is changed from 0 to 90 deg. Different types of faults are considered for several locations before and after series compensation. The obtained results are listed in Table II. The estimated ATWs for case 1, case 2 and case 7 are illustrated in Fig. 7 (a)-(C), respectively. From the table, it can be seen that the % error for each EFL is less than 1% which is within desired range. This certifies that proposed FLE approach is effective.

Additionally, the performance of the proposed approach is validated for faults at location of series compensation. As mentioned earlier, the compensation is provided at he middle of the line 1-5 i.e. 100 km from bus B1. The two faults are initiated at 100 km at 0.5 s just before and after compensation. The considered fault scenarios and results obtained from proposed approach are listed in Table III. The estimated ATWs for the two scenarios are depicted in Fig. 8. From the figure, it can be seen that estimated ATWs at two ends in both cases are exactly same. However, a close observation on the figure reveals that the magnitude of squared error is more when fault occurs after compensation in comparison to squared error obtained for fault occurring before compensation. Since, estimated ATWs are same for both cases, therefore, calculated fault locations and % errors are same. Aforementioned fact signifies that the approach accurately estimates fault location irrespective of fault located just before or after the series compensation.

TABLE II
PERFORMANCE UNDER DIFFERENT FAULT SCENARIOS

| | Case | Different fault scenarios | | | | EFL | %Error |
|---|---|---|---|---|---|---|---|
| | | Fault type | AFL (km) | FR (Ω) | FIA (deg.) | (km) | |
| Before compensation | 1. | AG | 12.50 | 0.01 | 0 | 12.1890 | 0.1554 |
| | 2. | AB | 21.20 | 1 | 30 | 20.6842 | 0.2579 |
| | 3. | ABG | 34.20 | 0.10 | 60 | 33.9620 | 0.1190 |
| | 4. | ABC | 62.80 | 1 | 90 | 62.4368 | 0.1816 |
| | 5. | ABCG | 81.30 | 5 | 30 | 81.6460 | 0.1731 |
| After compensation | 6. | AG | 105.40 | 0.10 | 30 | 105.1186 | 0.1407 |
| | 7. | AB | 114.30 | 0.01 | 0 | 114.0128 | 0.1436 |
| | 8. | ABG | 122.60 | 2 | 90 | 122.3274 | 0.1363 |
| | 9. | ABC | 150.70 | 0.01 | 0 | 150.74 | 0.0215 |
| | 10. | ABCG | 180.80 | 1 | 60 | 180.3628 | 0.2186 |

### B. *Performance for high resistance faults*

In general, high fault resistance deteriorates the performance of FLE. Therefore, the performance of proposed approach is investigated for aforementioned faults in this section. FRs

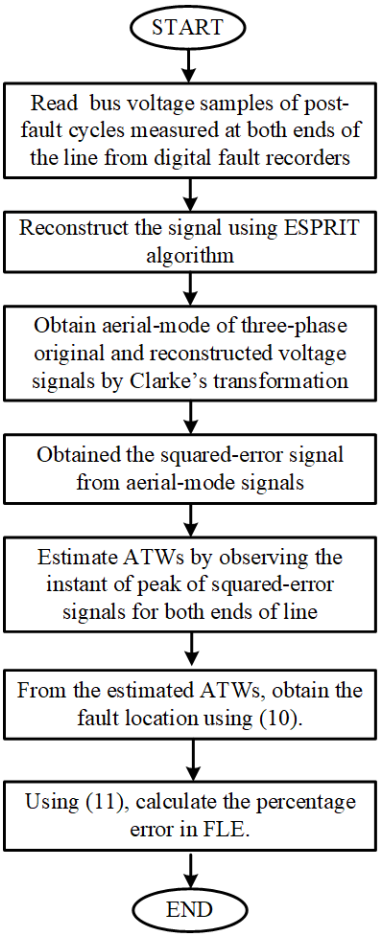


Fig. 6. Flowchart of proposed FLE approach.

TABLE III
PERFORMANCE UNDER FAULT AT LOCATION OF SERIES COMPENSATION

| | Fault type | AFL (km) | FR (Ω) | EFL (km) | % Error |
|---|---|---|---|---|---|
| Before compensation | ABCG | 100 | 0.01 | 98.92 | 0.5398 |
| After compensation | ABCG | 100 | 0.01 | 98.92 | 0.5398 |

are varied from 100 to 300 Ω. The considered cases along with obtained results are tabulated in Table IV. The estimated ATWs for case 1 and case 6 are shown in Fig. 9 (a) and (b), respectively. From the table, it can be noted that the proposed approach works satisfactorily well since % error in all cases are found to be less than 1%.

### C. Performance under TCSC compensation

To test the performance of proposed FLE approach with thyristor-controlled series capacitor (TCSC) compensation, a TCSC providing 50% compensation is connected in the middle of the line. The module of the TCSC with protection arrangement provided by metal-oxide varistor (MOV) and spark-gap is used in this work. The module is shown in Fig. 10. The numerical value of parameters of TCSC for providing

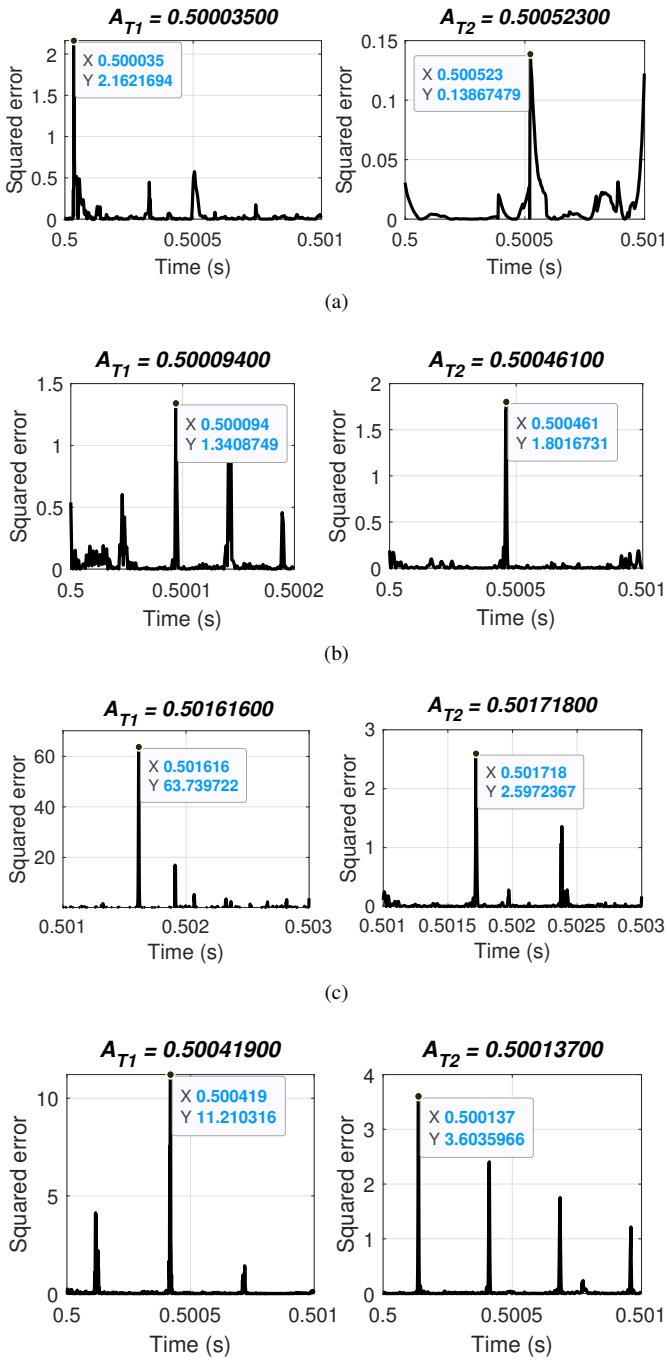


Fig. 7. Estimation of ATWs for different fault scenarios. (a) Case 1. (b) Case 3. (c) Case 5. (d) vase 9.

50% compensation to the line are $L_s$ = 23.518 mH and $C$ = 305 $\mu$F. TCSC is protected from over-voltage by MOV and spark-gap in this study. The voltage rating of MOV is considered to be 263.125 kV. The module provides smooth variable series capacitive/inductive reactance. The behavior of TCSC is similar to that of a parallel combination of variable inductor ($L_s$) and fixed capacitor ($C$). The equivalent impedance $Z_{eq}$ is given as

$$Z_{eq} = \left(\frac{j}{\omega C}\right)||(j\omega L_s) = \frac{-j}{\omega C - \frac{1}{\omega L}} \qquad (12)$$

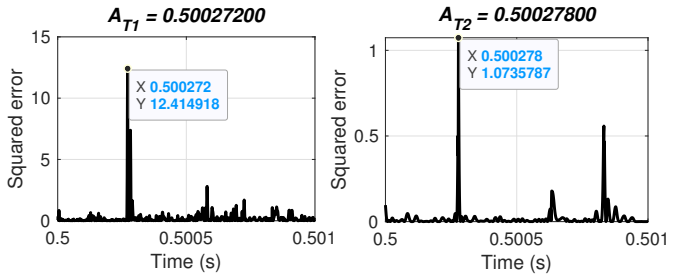


(a)

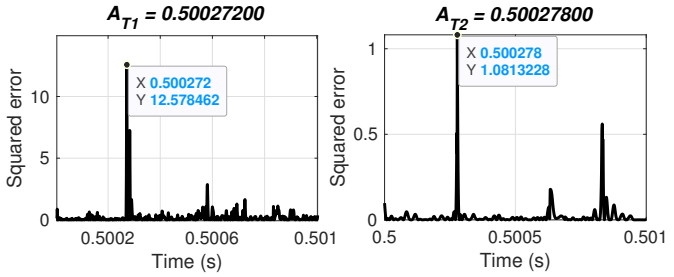


(b)

Fig. 8. Estimation of ATWs for fault at location of series compensation. (a) Before compensation. (b) After compensation.

TABLE IV
PERFORMANCE UNDER HIGH RESISTANCE FAULTS

| Case | Fault scenarios | | | EFL | %Error |
|---|---|---|---|---|---|
| | Fault type | AFL (km) | FR (Ω) | (km) | |
| 1. | AG | 25 | 100 | 24.7850 | 0.1074 |
| 2. | ABG | 50 | 200 | 49.0282 | 0.4859 |
| 3. | ABCG | 75 | 300 | 74.3240 | 0.3380 |
| 4. | AG | 120 | 100 | 119.3658 | 0.3171 |
| 5. | ABG | 145 | 200 | 144.2836 | 0.3582 |
| 6. | ABCG | 165 | 300 | 163.1600 | 0.9205 |

When $\omega C - \frac{1}{\omega L} > 0$, then TCSC provides variable capacitive reactance and when $\omega C - \frac{1}{\omega L} < 0$, then TCSC provides variable inductive reactance.

The considered cases and obtained results to validate the performance of proposed FLE approach under TCSC compensation are tabulated in Table V. The estimated ATWs for case 5 is depicted in Fig. 11. From the tabulated results, it can be concluded that proposed approach effectively locate the faults since % error in all cases are found to be less that acceptable limit of 1%.

### *D. Performance of proposed FLE approach for different location of TCSC compensation*

In this section, the performance of proposed FLE approach is validated for different TCSC locations. In all cases, a three-phase-to-ground fault is initiated on line 1-5 at 0.5 s. Three different locations of TCSC are considered for simulation i.e. sending-end i.e. bus B1, middle of the line i.e. 100 km from bus B1 and receiving-end i.e. bus B2. The obtained results are tabulated in Table VI. ATWs for all cases are estimated by proposed algorithm and are illustrated in Fig. 12. From the tabulated results, it can be observed that

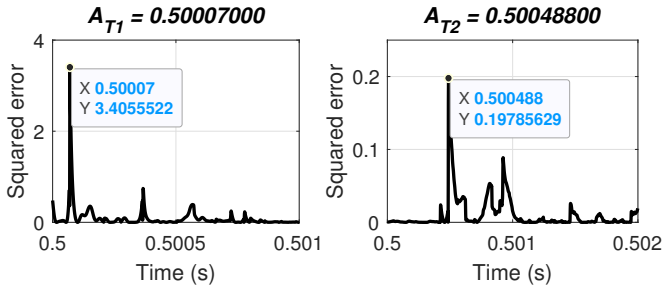


(a)

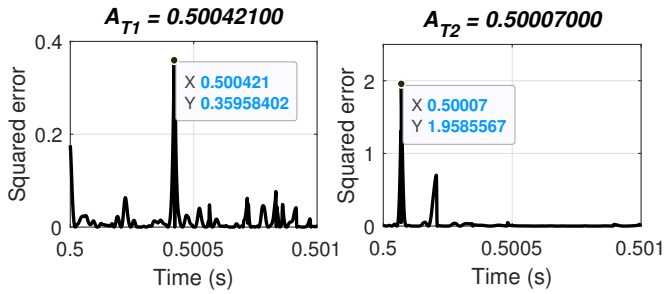


(b)

Fig. 9. Estimation of ATWs for high resistance faults. (a) Case 1. (b) Case 6.

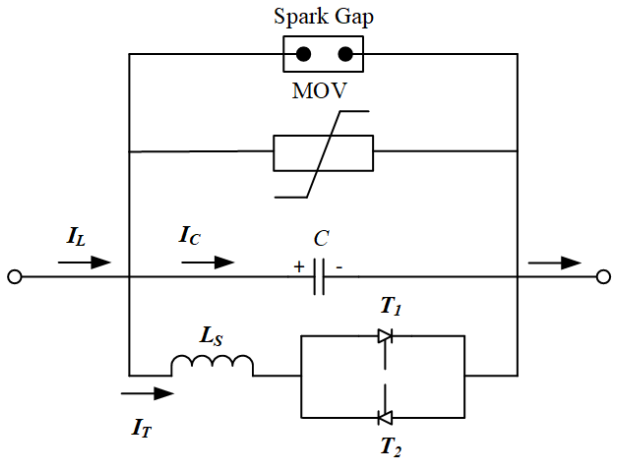


Fig. 10. Module of TCSC with protection arrangement.

TABLE V
PERFORMANCE UNDER TCSC COMPENSATION

| Case | Fault scenarios | | | EFL | % Error |
|---|---|---|---|---|---|
| | Fault type | AFL (km) | FR (Ω) | (km) | |
| 1. | AG | 30 | 0.01 | 29.6294 | 0.1853 |
| 2. | ABG | 55 | 1 | 54.2574 | 0.3713 |
| 3. | ABCG | 80 | 0.1 | 79.7856 | 0.1072 |
| 4. | AG | 130 | 0.01 | 129.3428 | 03282 |
| 5. | ABG | 165 | 1 | 163.3400 | 0.8305 |
| 6. | ABCG | 180 | 0.1 | 179.0852 | 0.4574 |

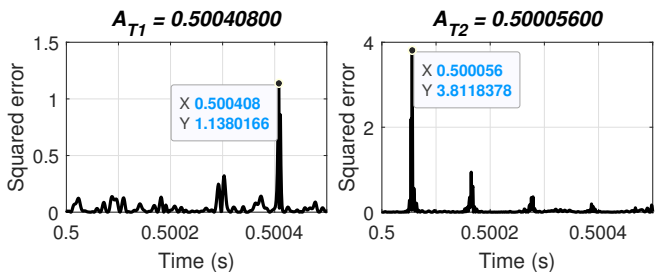


Fig. 11. Estimated ATWs for Case 5 under TCSC compensation.

TABLE VI
PERFORMANCE UNDER DIFFERENT LOCATION OF TCSC COMPENSATION

| Case | TCSC location | AFL (km) | EFL (km) | % Error |
|---|---|---|---|---|
| 1. | Sending-end | 70 | 71.0300 | 0.5148 |
| 2. | Mid-point | 80 | 80.2070 | 0.1033 |
| 3. | Mid-point | 120 | 120.3300 | 0.1666 |
| 4. | Receiving-end | 130 | 130.0500 | 0.0250 |

TABLE VII
PERFORMANCE UNDER DIFFERENT SIGNAL TO NOISE RATIO (SNR)

| Case | SNR (db) | AFL (km) | EFL (km) | % Error |
|---|---|---|---|---|
| 1. | No noise | 150.70 | 150.74 | 0.0215 |
| 2. | 40 | 150.70 | 150.92 | 0.1115 |
| 3. | 30 | 150.70 | 151.10 | 0.2015 |
| 4. | 20 | 150.70 | 151.20 | 0.2484 |

the proposed method works efficiently in localizing faults irrespective of change in the location of TCSC compensation.

### *E. Performance of proposed FLE approach for signals with noise*

In this section, the performance of proposed FLE approach is validated for different levels of noise in the signal. For simulation, a three-phase fault is initiated at 150.70 km from bus B1 on line 1-5 at 0.5 s. A signal-to-noise (SNR) value is varied from 40 db to 20 db. The obtained results are tabulated in Table VII. The estimated ATWs from proposed approach are depicted in Fig. 13. From the results listed in the table, it can be inferred that the proposed method works well in case of signals contaminated with noise. However, it is worthy to note here that with increase in the levels of noise, the performance of the approach deteriorates i.e. the value of % error increases.

### *F. Comparative assessment with existing techniques*

In this section, qualitative and quantitative comparative assessments of proposed FLE approach with existing approaches are presented. The performance of proposed method is compared with FLE approaches based on S-transform (ST) [31], empirical mode decomposition (EMD) [32] and variational mode decomposition (VMD) [6]. To validate the performance, a three-phase-to-ground (ABCG) fault is initiated at 140 km from bus B1 on line 1-5 with series compensation provided at 100 km. The fault inception time is 0.5 s. The obtained results for the considered case is listed in

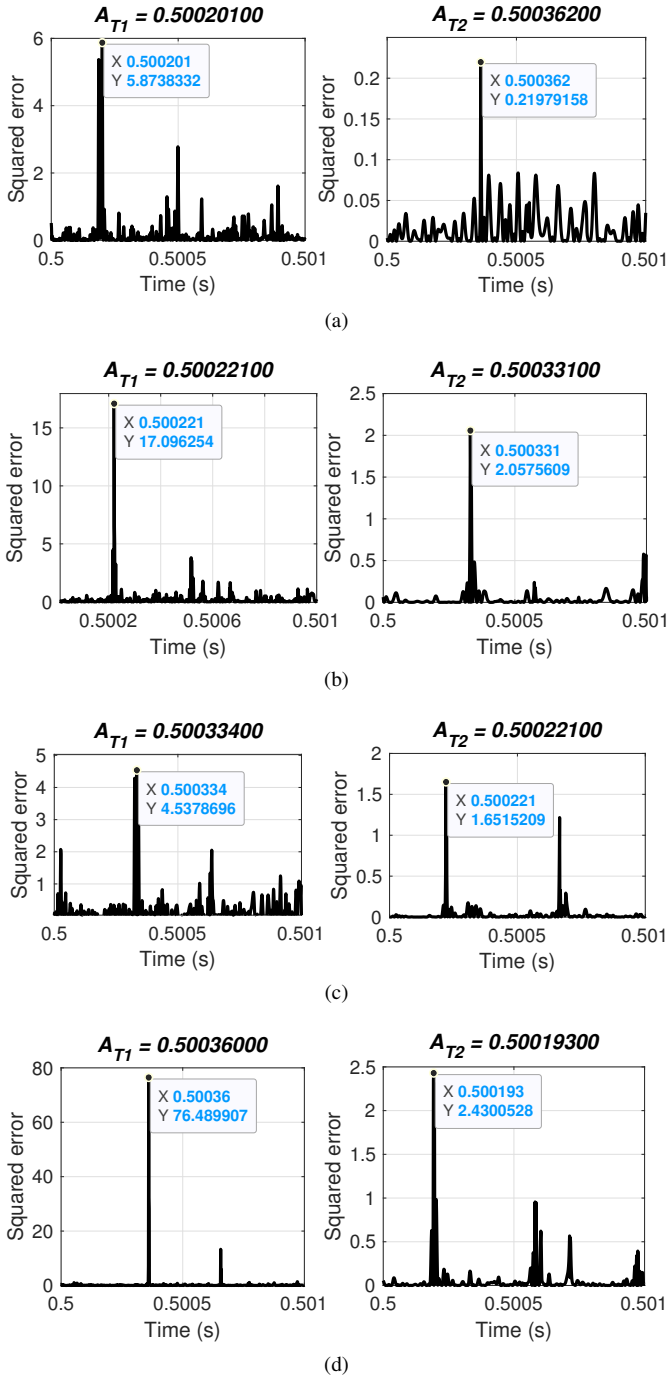


Fig. 12. Estimation of ATWs for different TCSC locations. (a) Case 1. (b) Case 2. (c) Case 3. (d) Case 4.

Table VIII. The estimated ATWs from the different methods are presented ib Fig. 14. From the figure, it can be seen that proposed method accurately estimates ATWs than others which eventually produces minimum % error in calculation of fault location (see Table VIII ). It is worthy to note here that the performance of other three methods, ST, EMD and VMD are similar to each other.

The quantitative comparison is listed in Table IX. From the table, it can be observed that the proposed FLE approach is the only approach applied to FSC or TCSC compensated lines connected to wind farms. Additionally, only voltage

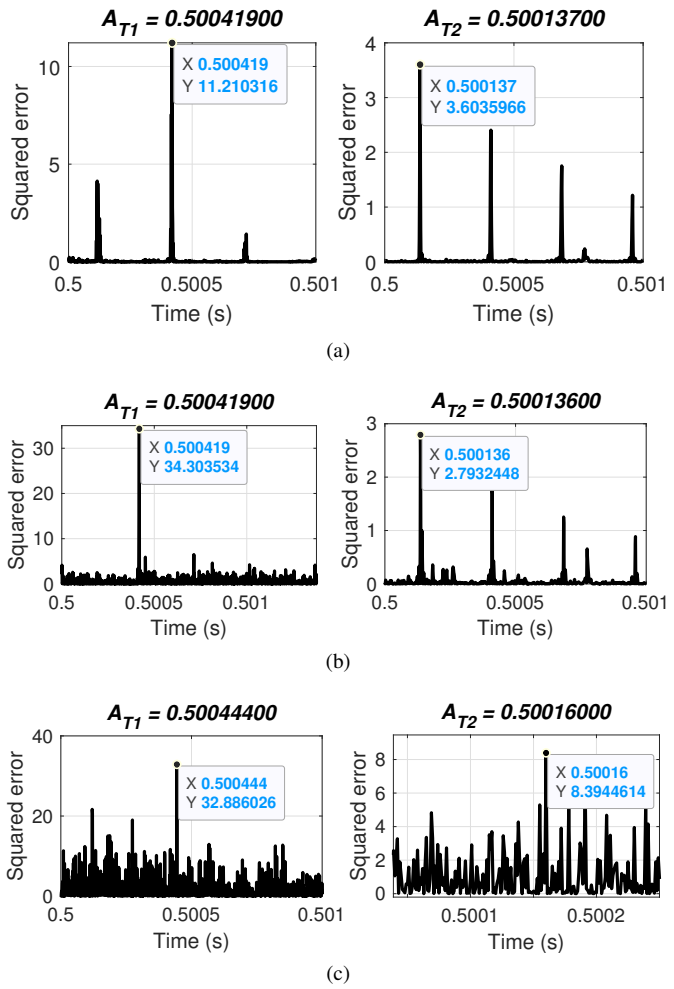


Fig. 13. Estimation of ATWs for different SNRs. (a) Case 1. (b) Case 2. (c) Case 3.

TABLE VIII
QUALITATIVE COMPARATIVE ASSESSMENT OF PROPOSED FLE APPROACH

| Method | Fault type | AFL (km) | EFL (km) | % Error |
|---|---|---|---|---|
| ST [31] | ABCG | 140 | 139.5868 | 0.2066 |
| EMD [32] | ABCG | 140 | 139.5868 | 0.2066 |
| VMD [6] | ABCG | 140 | 139.5868 | 0.2066 |
| Proposed | ABCG | 140 | 139.9500 | 0.0266 |

signals are utilized by proposed work as input signal while others use either current signal or both signals. It is worthy to mention here that current signals are more susceptible to transient phenomena than voltage signals and thus, may produce erroneous results if used.

## VII. CONCLUSION

In present work, a novel approach to locate faults in series compensated line connected to wind farms is introduced. The proposed FLE approach is based on extracting ATWs from peak of squared-error signal from post-fault samples. At first, the original signal is reconstructed via ESPRIT algorithm and then, the aerial-modes of original and reconstructed

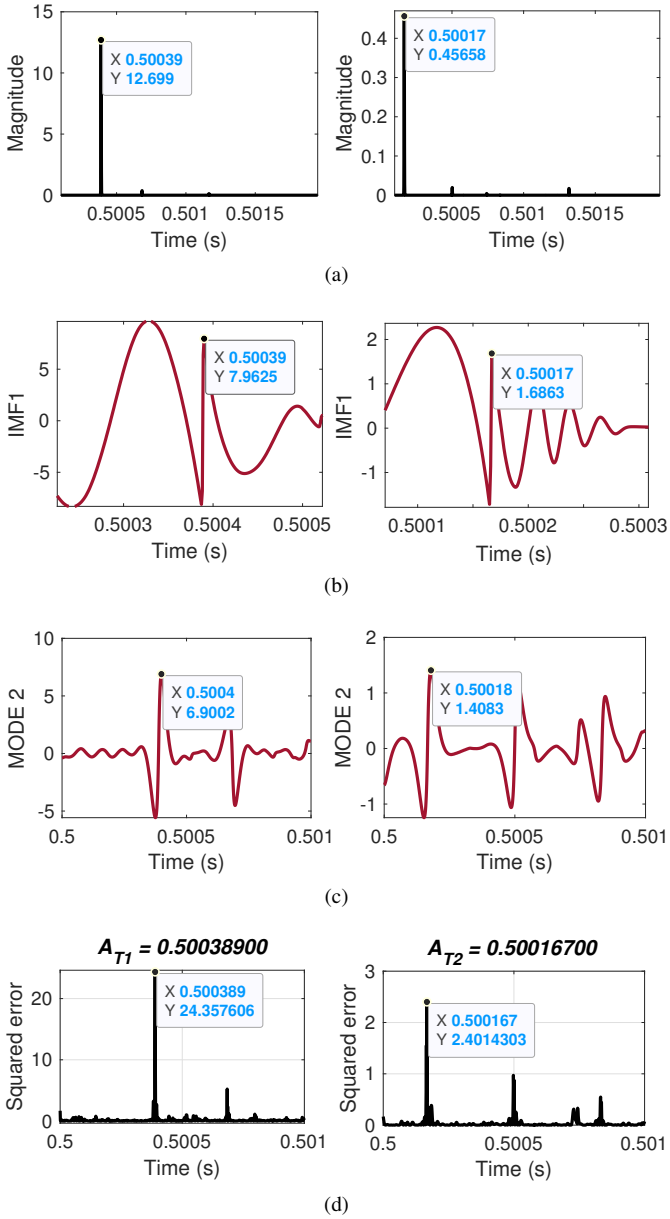


Fig. 14. Estimation of ATWs from different methods. (a) ST. (b) EMD. (c) VMD. (d) Proposed.

signals are obtained. The error signal is formed by taking the difference between aerial-mode signals. From the studied results, following major conclusions can be drawn.

- The proposed FLE approach is insensitive towards the fault location before or after series compensation.
- The accuracy of FLE approach is not affected by system parameters variations like FRs, FIAs and types of faults.
- The approach is found to be robust for high resistance faults.
- TCSC compensation in place of FSC compensation is least affecting the performance of the proposed approach.
- Location of TCSC installation does not affect the performance of the algorithm.
- The proposed approach performs efficiently for signals with noises.
- Presented FLE algorithm is comparatively better than

TABLE IX
COMPARATIVE ASSESSMENT OF PROPOSED FLE APPROACH

| FLE approach | Type of method | Input signal | Type of compensation |
|---|---|---|---|
| FDST [4] | Traveling-wave based FLE | Current signal | TCSC and wind farm |
| Conventional algorithm [7] | Impedance based FLE | Voltage and current signals | Wind farm |
| ANN and WT [10] | Artificial intelligence based FLE | Voltage and current signals | TCSC |
| ANN [11] | Artificial intelligence based FLE | Voltage and current signals | FSC |
| DWT and decision tree [12] | Artificial intelligence based FLE | Voltage and current signals | FSC |
| EMD and random forest [20] | Hybrid method based FLE | Current signal | TCSC and wind farm |
| Proposed | Traveling-wave based FLE | Voltage signal | FSC, TCSC and wind farm |

existing techniques in localization of faults in series compensated line connected to wind farms.

In this work, two-terminal instantaneous voltage signals are used for FLE. The validity of proposed approach will be tested with one-end signal in future. Further, the validity of presented approach will be investigated for more complex power systems including double-circuit lines.

## REFERENCES


[1] X.-F. Wang, Y. Song, and M. Irving, *Modern power systems analysis*. Springer Science & Business Media, 2010.

[2] T. Ackermann, *Wind power in power systems*. John Wiley & Sons, 2005.

[3] L. Piyasinghe, Z. Miao, J. Khazaei, and L. Fan, "Impedance model-based ssr analysis for tcsc compensated type-3 wind energy delivery systems," *IEEE Transactions on Sustainable Energy*, vol. 6, no. 1, pp. 179–187, 2014.

[4] B. Sahoo and S. R. Samantaray, "An enhanced fault detection and location estimation method for tcsc compensated line connecting wind farm," *International Journal of Electrical Power & Energy Systems*, vol. 96, pp. 432–441, 2018.

[5] N. Rezaei, M. Uddin, K. A. Ifte, M. L. Othman, M. Marsadek, and M. M. Hasan, "A novel hybrid machine learning classifier based digital differential protection scheme for intertie zone of large-scale centralized dfig based wind farms," *IEEE Transactions on Industry Applications*, 2020.

[6] S. Mishra, S. Gupta, and A. Yadav, "Intrinsic time decomposition based fault location scheme for unified power flow controller compensated transmission line," *International Transactions on Electrical Energy Systems*, p. e12585, 2020.

[7] M. M. M. Aly and M. A. El-Sayed, "Enhanced fault location algorithm for smart grid containing wind farm using wireless communication facilities," *IET Generation, Transmission & Distribution*, vol. 10, no. 9, pp. 2231–2239, 2016.

[8] P. Kundu and A. K. Pradhan, "Real-time analysis of power system protection schemes using synchronized data," *IEEE Transactions on Industrial Informatics*, vol. 14, no. 9, pp. 3831–3839, 2018.

[9] M. Pazoki, "A new fault classifier in transmission lines using intrinsic time decomposition," *IEEE Transactions on Industrial Informatics*, vol. 14, no. 2, pp. 619–628, 2017.

[10] A. Swetapadma and A. Yadav, "Improved fault location algorithm for multi-location faults, transforming faults and shunt faults in thyristor controlled series capacitor compensated transmission line," *IET Generation, Transmission & Distribution*, vol. 9, no. 13, pp. 1597–1607, 2015.

[11] A. Swetapadma and A. Yadav, "An artificial neural network-based solution to locate the multilocation faults in double circuit series capacitor compensated transmission lines," *International Transactions on Electrical Energy Systems*, vol. 28, no. 4, p. e2517, 2018.

[12] A. Swetapadma and A. Yadav, "A hybrid method for fault location estimation in a fixed series compensated lines," *Measurement*, vol. 123, pp. 8–18, 2018.

[13] P. K. Mishra, A. Yadav, and M. Pazoki, "Fdost-based fault classification scheme for fixed series compensated transmission system," *IEEE Systems Journal*, vol. 13, no. 3, pp. 3316–3325, 2019.

[14] P. K. Mishra, A. Yadav, and M. Pazoki, "Resilience-oriented protection scheme for tcsc-compensated line," *International Journal of Electrical Power & Energy Systems*, vol. 121, p. 106103, 2020.

[15] F. C. A. Fernandes, R. L. C. van Spaendonck, and C. S. Burrus, "A new framework for complex wavelet transforms," *IEEE Transactions on Signal Processing*, vol. 51, no. 7, pp. 1825–1837, 2003.

[16] M. Nemati, M. Bigdeli, A. Ghorbani, and H. Mehrjerdi, "Accurate fault location element for series compensated double-circuit transmission lines utilizing negative-sequence phasors," *Electric Power Systems Research*, vol. 194, p. 107064, 2021.

[17] A. Saber, "Adaptive fast protection technique for uncompensated/compensated double-circuit transmission lines connected to large-scale wind farms," *IET Renewable Power Generation*, vol. 14, no. 13, pp. 2315–2322, 2020.

[18] H. Sadeghi, "A novel method for adaptive distance protection of transmission line connected to wind farms," *International Journal of Electrical Power & Energy Systems*, vol. 43, no. 1, pp. 1376–1382, 2012.

[19] N. Perera and A. D. Rajapakse, "Series-compensated double-circuit transmission-line protection using directions of current transients," *IEEE Transactions on power delivery*, vol. 28, no. 3, pp. 1566–1575, 2013.

[20] S. Biswas and P. K. Nayak, "A new approach for protecting tcsc compensated transmission lines connected to dfig-based wind farm," *IEEE Transactions on Industrial Informatics*, 2020.

[21] S. Chen, N. Tai, C. Fan, J. Liu, and S. Hong, "Adaptive distance protection for grounded fault of lines connected with doubly-fed induction generators," *IET Generation, Transmission & Distribution*, vol. 11, no. 6, pp. 1513–1520, 2017.

[22] C. D. Prasad and M. Biswal, "Swarm intelligence-based differential protection scheme for wind integrated transmission system," *Computers & Electrical Engineering*, vol. 86, p. 106709, 2020.

[23] A. Hooshyar, M. A. Azzouz, and E. F. El-Saadany, "Distance protection of lines connected to induction generator-based wind farms during balanced faults," *IEEE Transactions on Sustainable Energy*, vol. 5, no. 4, pp. 1193–1203, 2014.

[24] Y. Chen, M. Wen, X. Yin, Y. Cai, and J. Zheng, "Distance protection for transmission lines of dfig-based wind power integration system," *International Journal of Electrical Power & Energy Systems*, vol. 100, pp. 438–448, 2018.

[25] B. Li, J. Liu, X. Wang, and L. Zhao, "Fault studies and distance protection of transmission lines connected to dfig-based wind farms," *Applied Sciences*, vol. 8, no. 4, p. 562, 2018.

[26] X. Chen, X. Yin, and Z. Zhang, "Impacts of dfig-based wind farm integration on its tie line distance protection and countermeasures," *IEEJ Transactions on Electrical and Electronic Engineering*, vol. 12, no. 4, pp. 553–564, 2017.

[27] M. A. Aftab, S. S. Hussain, I. Ali, and T. S. Ustun, "Dynamic protection of power systems with high penetration of renewables: A review of the traveling wave based fault location techniques," *International Journal of Electrical Power & Energy Systems*, vol. 114, p. 105410, 2020.

[28] R. Roy and T. Kailath, "Esprit-estimation of signal parameters via rotational invariance techniques," *IEEE Transactions on acoustics, speech, and signal processing*, vol. 37, no. 7, pp. 984–995, 1989.

[29] E. Santos, M. Khosravy, M. A. Lima, A. S. Cerqueira, and C. A. Duque, "Esprit associated with filter bank for power-line harmonics, sub-harmonics and inter-harmonics parameters estimation," *International Journal of Electrical Power & Energy Systems*, vol. 118, p. 105731, 2020.

[30] A. J. Conejo, F. D. Galiana, and I. Kockar, "Z-bus loss allocation," *IEEE Transactions on Power Systems*, vol. 16, no. 1, pp. 105–110, 2001.

[31] B. Chaitanya and A. Yadav, "Decision tree aided travelling wave based fault section identification and location scheme for multi-terminal transmission lines," *Measurement*, vol. 135, pp. 312–322, 2019.

[32] S. Mishra, S. Gupta, and A. Yadav, "Empirical mode decomposition assisted fault localization for upfc compensated system," in *2020 21st National Power Systems Conference (NPSC)*. IEEE, 2020, pp. 1–6.